Towards Mobile and Touchless Fingerprint Verification

Christof Jonietz[1], Eduardo Monari[1], Heiko Widak[1], Chengchao Qu[2,1]
[1]Fraunhofer IOSB
Fraunhoferstr. 1, 76131 Karlsruhe, Germany
[2]Vision and Fusion Laboratory (IES), Karlsruhe Institute of Technology (KIT)
Adenauerring 4, 76131 Karlsruhe, Germany
{firstname.lastname}@iosb.fraunhofer.de

Abstract

Touchless finger detection for the biometric fingerprint verification/identification process with mobile devices is considered in this paper. Fingerprint capturing is based on a camera system with bright-field illumination. For finger detection, a machine learning based algorithm with Aggregated Channel Features (ACFs) and a skin-color based finger segmentation with a geometric shape based approach for fingertip detection are considered, respectively. Results demonstrate the performance of both algorithms.

1. Introduction

The project *MobilePass* [2] focuses on research and development towards technologically advanced mobile equipment at land border crossing points. This will allow border control authorities to check European, visa-holding and frequent third country travelers in a comfortable, fast and secure way. The mobile solution incorporates new technologies for mobile scenarios and integrates them in the actual border crossing workflow to speed up control procedures. Here, contactless finger detection for biometric fingerprint verification/identification process with mobile devices is considered.

Several approaches for finger detection with different sensors are discussed in the literature. In [11, 10, 16], finger detection is based on the top-hat transform, which uses morphological operators on a hand blob by subtracting the results from the original hand blob. However, a reliable segmentation of the RGB image is a prerequisite of many algorithms that analyze a binary blob image and the performance of these algorithms crucially depends on the segmentation result. In [11], color segmentation is performed in YUV color space. In [17], a shape representation based on time-series curve is used for fingertip detection. In [3], a skeleton-based approach is proposed for fingertip detection.

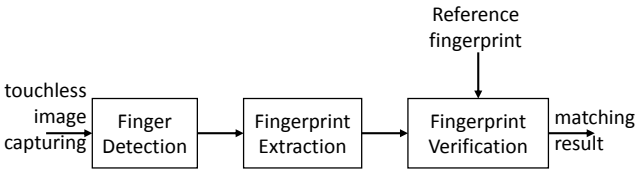

Figure 1: Processing chain.

In this paper, we focus on touchless capturing of fingertips. As a requirement for the capturing device, the resolution of the sensor should be such, that each fingerprint image can be cropped with a resolution of at least 500 dots per inch (DPI), which is the minimum resolution in a fingerprint verification/identification process. A machine learning based algorithm with ACFs adopted for finger detection is considered.

The processing workflow is depicted in Fig. 1. In the first steps, the whole finger is captured by a camera. Based on the detected fingertip the fingerprint image is extracted in order to perform fingerprint verification.

This paper is organized as follows. In Sec. 2, the camera system with bright-light illumination suitable for fingerprint capturing is described. In Sec. 3 and Sec. 4, the finger detector based on ACF and finger segmentation with geometric shape based fingertip detection is proposed, respectively. In Sec. 5 and Sec. 6 results are presented and conclusions are drawn, respectively.

2. Capturing System

One of the critical elements of the future *MobilePass* device is the camera system. For a mobile device weight and size is very important. The function of the camera is to capture images of fingerprints with resolution sufficient to extract minutias with high quality, which is one of the major features of a fingerprint that allows comparison with other fingerprints.

The UI-3013XC camera from IDS [1] with artificial

Figure 2: Camera and LED's arranged to a bright-field illumination.

Figure 3: Result of a fingerprint image with bright-field illumination.

illumination is used for fingerprint image capturing, cf. Fig. 2. Bright-field illumination is the most commonly used method to illuminate rough surfaces, such as fingerprints. Due to the arrangement of the LED's close to the optical axis, the surface is bright. Valleys in the fingerprints texture appear as dark curve, cf. Fig. 3. The minimum resolution of the image raw data should be approximately 500 DPI for fingerprint images and the UI-3013XC delivers a Full-HD (1920×1080 pixel) images in video mode with a frame rate of 30 frames per second (fps), which is sufficient for this application.

The *MobilePass* system might be used indoors (trains, buses, buildings) as well as in outdoor scenarios. Hence, very high contrast variations will occur during the capturing process. The camera has a built-in compensation for backlight illumination. Since there is no fixed connection between the scanned object and the imaging device there is a lot of motion between both. The camera should use fast exposure modes for sharp images and low motion blur. It is essential for the camera system to be operated in a mode where the fast shutter is given priority over the gain control. Due to the additional illumination, the camera system can be operated in shutter priority mode in order to avoid motion blur. For low maintenance a durable illumination system is of advantage. This could be provided by a customized LED illumination. Highlights should be avoided for a maximum ambient light distribution high power LED with a wide dissemination angel should be chosen. Controlled illumination intensity and Pulse Width Modulated (PWM) mechanisms are suitable. The main advantage of PWM is power loss in the switching devices is very low. In addition, it allows a wide operating range by varying power on and off duty cycles. The light control mechanism should have the possibility to synchronize with the camera system and the reaction time should be faster than the frame rate to allow an illumination change immediately after calculations (e.g. histograms) from the last captured frame. The arrangement of light emitting elements should provide maximum ambient light conditions for uniform illumination. To increase the contrast and thus to enhance topographic details of a fingerprint image, the high power LED's should be arranged close to the optical axis of the camera to use the effects of a bright-field illumination, cf. Fig. 2.

3. ACF Finger Detector

Following the footsteps of Histograms of Oriented Gradients (HOG) by Dalal and Triggs [5] in 2005, combining rich feature descriptors and effective learning methods has become the standard technique to detect rigid objects from image data. In the recent researches, a new family of features—the Integral Channel Features (ICF)—proved to be highly discriminative leveraging complementary color and gradient channels [8]. By replacing the rectangular integral images in ICF with the sum of small squares, Dollár et al. proposed the state-of-the-art Aggregated Channel Feature (ACF) algorithm [6], which approximated multiscale HOG instead of dense image of classifier pyramid to achieve real-time detection [7].

Despite the articulation of fingers, the detection in the context of *MobilePass* can still be categorized into rigid object detection, because with the constrained recording condition, the subjects are guided to show upright fingers in front of the camera, analog to the upper body of pedestrians. Considering such similarity, we explore the viability of employing ACF for detection fingers.

Features. In [8], Dollár et al. systematically evaluated various combinations of feature channels as well as learning algorithms and showed the effectiveness of employing LUV color channels in addition to the gradient magnitude and 6 HOG channels, yielding 10 channels in total. Gaussian filtering is applied before and after aggregating the 4×4 pixel blocks. Fig. 4 illustrates an example of the computed ACFs. The compact description by aggregated features is able to further boost the efficiency of the algorithm without loss of representation power. Moreover, the person-specific inner textural information of the finger is smoothed out.

Multiscale ACF Approximation. Instead of applying the dense sliding window routine to the multiscale image pyramid and computing features for dozens of times on it, Dollár et al. [7, 6] proposed to adapt ACF to different scale spaces. Since resizing of color channels is trivial, specific resampling scheme for the HOG features is needed. Inspired by the power law when scaling natural images [18] with regard to the ratio of scales, ACF channels $\mathbf{f}_{\mathbf{\Omega}}(\mathbf{I}_{s_1})$ of image $\mathbf{I}$ in an arbitrary scale s_1 are subject to a simple recalculation of

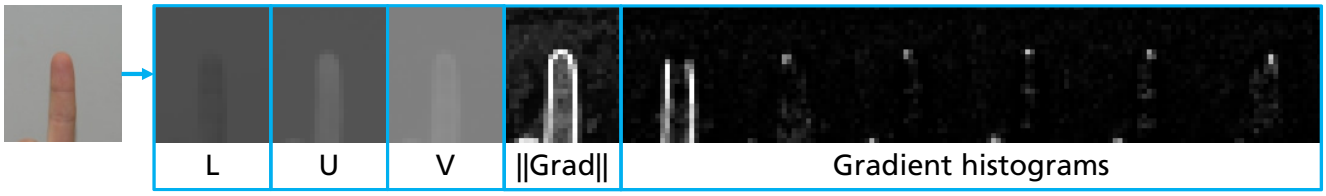

Figure 4: Illustration of the computed ACF from an example fingertip image.

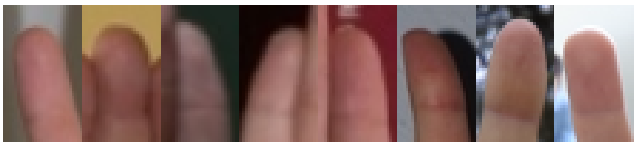

Figure 5: Example images of our dataset for training the ACF fingertip detector.

that in the original scale space s_0

$$\mathbf{f}_{\mathbf{\Omega}}(\mathbf{I}_{s_1}) = \mathbf{f}_{\mathbf{\Omega}}(\mathbf{I}_{s_0}) \cdot \left(\frac{s_1}{s_0}\right)^{-\lambda_{\mathbf{\Omega}}}, \qquad (1)$$

where $\mathbf{f}_{\mathbf{\Omega}}$ refers to the channel feature $\mathbf{\Omega}$ with its own corresponding scale factor $\lambda_{\mathbf{\Omega}}$, which can be obtained by statistical learning from the training images. The benefit lies in that the rich image features are extracted as few times as possible, addressing the performance drawback of the traditional sliding window pipeline with an ideal trade-off between accuracy and speed.

Training. In spite of the numerous hand and gesture datasets in the research community, hands with arbitrary posture are not suitable to the training of upright ACF finger detector. We collected approximately 2000 finger crops out of 500 images from 3 publicly available datasets, i.e. the Sébastien Marcel Static Hand Posture Database[1] [13], the Database for Hand Gesture Recognition[2] [15], and the hand gesture dataset acquired with Leap Motion and the Kinect devices[3] [14], as well as using the *MobilePass* capturing system for better adaptation to the deployment condition. Some of the samples resized to 20×40 pixels for training are depicted in Fig. 5. Note that challenges such as orientation variation and partial occlusion caused by finger clustering are widely present in the dataset.

4. Finger Detection by Edge Pairing

In the following, a fingertip detection algorithm is proposed based on evaluation of the segmented finger. The main idea is to associate the "left" and "right" edges to a finger through edge-pairing and to extract it by its respective tip and angle. The edge-pairing algorithm is subdivided into the following steps: (1) finger segmentation, (2) converting the binary blob image into a contour line, (3) locating line segments within the contour line, and (4) forming fingers by pairing edges.

Finger segmentation. One straight forward approach for segmentation of body parts is using skin color. In literature, several approaches exist which mainly try to detect pixels with human skin tones, without any prior knowledge on images content [12, 9]. However, due to the applied finger detection step as pre-processing, in our case skin color estimation and segmentation can be designed in a more robust way. For pixel-based skin color detection, we use the algorithms proposed in [4]. This segmentation step allows for sub-sequential shape analysis of the finger, and as a consequence to search for fingertips, cf. Fig. 6a.

Converting the Binary Blob Image into a Contour Line. In order to process and examine the blobs contained in the binary input image (Fig. 6b) efficiently, the blobs are converted into contour lines, cf. Fig. 6c. A contour is a sequence of pixels located along the boundaries of the blob. If there are several disconnected blobs in an input image (e.g. only fingers visible), multiple contours are computed and processed separately from each another.

Line Segmentation of the Contour Line. The most important recognition features of a finger are approximately long lines along it. In order to detect such lines and deduce the presence of a finger, it is necessary to isolate them from the contour line of a blob by isolating line segments within a contour. Line segments are detected by analyzing the variation of the tangent angle on the contour. Within a line segment the variation is low, i.e. the tangent angle remains almost constant. In order to detect line segments a set of seed points is computed. Seed points are candidates points on a contour to start on when trying to detect a line segment. The seed point list is defined by contour points having a small difference of their bilateral tangential angles. Since line segments usually consist of many consecutive seed points, the

[1] http://www.idiap.ch/resource/gestures/
[2] http://sun.aei.polsl.pl/~mkawulok/gestures/
[3] http://lttm.dei.unipd.it/downloads/gesture/

seed point list is filtered by picking only one (the middle) of all consecutively seed points observed on a contour. After the contour line has been segmented, the orientation is calculated for the isolated line segments.

Forming fingers by matching edges. The formation of fingers based on the previously computed line segments is provided by edge pairing. A pair of edges is consequently interpreted as the "left" and "right" edge of the finger. The method is illustrated in Fig. 6d, where the line segments used for reconstruction of paired edges are plotted in the same color. An edge can only be combined with another edge. Unpaired edges are discarded and are not recognized as a finger. In order to find the best match for each edge, a match quality metric for a hypothetical pair of edges is calculated, which depends on the orientation of edges, the distance between center points, the maximum allowed pairing angle, and the length of edges. An hypothetical edge pair that fulfills the quality criterion is denoted as edge pair.

5. Results

In this section, quantitative and qualitative evaluations of the employed finger detection algorithms are carried out. In addition to ACF and Edge Pairing, the classic HOG detector by Dalal and Triggs [5] was chosen as the baseline for the comparison, which was trained using the same data as ACF described in Sec. 3. In order to assess the feasibility of the deployed system, test images containing 4 subjectives of 3 indoor and outdoor scenarios are collected. In each test image, the test person was requested to show a single finger (except the thumb) of both hands, leading to totally 96 images. In order to compare the detection accuracies of the proposed algorithms, the region-of-interests (ROIs) of each finger, i.e. the desired fingertip for the fingerprint verification process, has manually been labeled by an rectangular window. In the following, these labeled ROIs are compared against the ROIs determined by the proposed algorithms.

(a) Input RGB image.

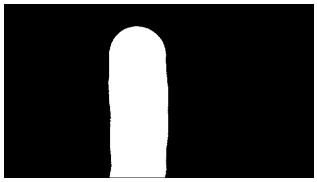

(b) Segmented finger.

(c) Contour image with line segments.

(d) Edge image with normal vectors.

Figure 6: Finger detection by edge pairing.

The Receiver Operating Characteristic (ROC) curve of ACF and the corresponding results of HOG and Edge Pairing are depicted in Fig. 7. By virtue of the bright-field illumination concept, the fingers are uniformly illuminated, which clearly stands out even in outdoor scenes. Another advantage of the recording system lies in that the fingers are relatively close to the camera, which makes the background objects with a much larger distance, e.g., the ground and feet, out of focus. The two-fold convenience allows ACF to perform much better than in the pedestrian detection task. Less than 2% miss rate with 0.1 false positive per image (FPPI) is a order of magnitude better than HOG. On the other hand, the data point of Edge Pairing is actually invisible on the plot, since zero FPPI is obtained thanks to the well-designed segmentation algorithm. Only one missed detection means the miss rate is merely 1%, which achieves the absolutely best result among the three approaches.

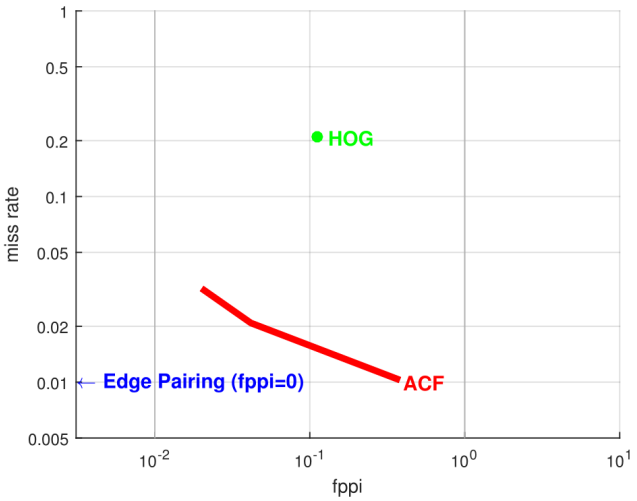

Figure 7: ROC curve of finger detection on the test data using HOG (green), ACF (red) and Edge Pairing (blue).

Fig. 8 offers a qualitative comparison of the ROIs generated by the evaluated methods. Because only grayscale information is taken into account in HOG, the similarly shaped foot and the brick on the ground are sometimes also misleadingly classified as a false positive. ACF detects small ROI near the edge of skin area where the true fingertip is not present. However, it is worth a mention that the confidence score is relatively low compared to the true finger, which can be removed by using a higher threshold (than zero here in the images) via cross-validation. Moreover, those small false positives can be further circumvented by only allowing an appropriate ROI size. Last but not least, with the help of the segmentation algorithm, Edge Pairing

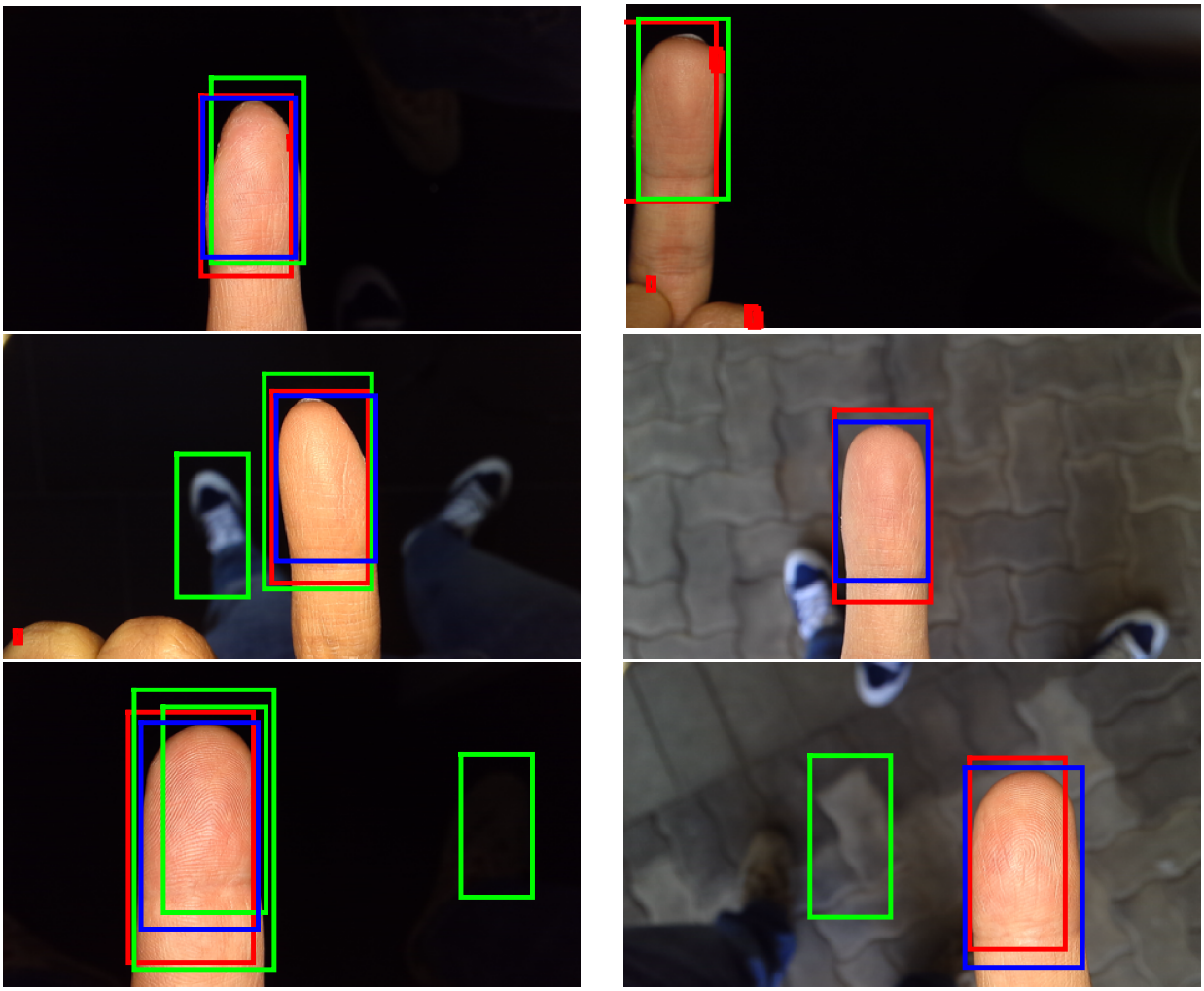

Figure 8: Examples of the detected ROIs from the test data using HOG (green), ACF (red) and Edge Pairing (blue).

crops the most precise ROIs, which is not reflected in the ROC plot in Fig. 7.

Method	Overlap
ACF	0.7591 ± 0.0750
Edge Pairing	0.8437 ± 0.0382

Table 1: Overlap of the detected ROIs with the ground truth ROIs.

A preferably tight, accurate and stable ROI is considered advantageous for fingerprint verification. To further investigate this case quantitatively, the overlap of the detected ROIs using ACF and Edge Pairing with the ground truth ROIs is listed in Tab. 1, where the mean overlap with standard deviation of the true-positive detections are given. The qualitative benefit of Edge Pairing in Fig. 8 is justified in numbers with nearly 10% higher overlap and doubled stability of its ROIs.

6. Conclusions

In this paper, touchless finger detection for the biometric fingerprint recognition process has been considered. A prototype camera system with bright-field illumination has been presented, which is especially suitable for fingerprint capturing. A machine learning based algorithm with ACFs and a geometric shape approach based on evaluating the contour of the segmented finger are considered for fingertip detection. An evaluation based on a measurement campaign in different indoor and outdoor scenarios demonstrate the suitability of the geometric approach by edge pairing in extracting fingertips for a biometric identification/verification process.

7. Acknowledgment

This project has received funding from the European Union's Seventh Framework program for research, technological development and demonstration under grant agreement No. 608016.

References

[1] Datasheet IDS UI-3013XC. available on https://en.ids-imaging.com. 1

[2] http://mobilepass-project.eu. 1

[3] X. Bai, L. J. Latecki, and W. Liu. Skeleton pruning by contour partitioning with discrete curve evolution. *Pattern Analysis and Machine Intelligence, IEEE Transactions on*, 29(3):449–462, March 2007. 1

[4] A. Cheddad, J. Condell, K. Curran, and P. McKevitt. A new colour space for skin tone detection. In *Image Processing (ICIP), 2009 16th IEEE International Conference on*, pages 497–500, Nov 2009. 3

[5] N. Dalal and B. Triggs. Histograms of oriented gradients for human detection. In *Computer Vision and Pattern Recognition, 2005. CVPR 2005. IEEE Computer Society Conference on*, volume 1, pages 886–893, June 2005. 2, 4

[6] P. Dollár, R. Appel, S. Belongie, and P. Perona. Fast feature pyramids for object detection. *Pattern Analysis and Machine Intelligence, IEEE Transactions on*, 36(8):1532–1545, Aug 2014. 2

[7] P. Dollár, S. Belongie, and P. Perona. The fastest pedestrian detector in the west. In *Proceedings of the British Machine Vision Conference*, pages 68.1–68.11. BMVA Press, 2010. 2

[8] P. Dollár, Z. Tu, P. Perona, and S. Belongie. Integral channel features. In *Proceedings of the British Machine Vision Conference*, pages 91.1–91.11. BMVA Press, 2009. 2

[9] A. Farrukh, A. Ahmad, M. I. Khan, and N. Khan. Automated segmentation of skin-tone regions in video sequences. In *Students Conference, 2002. ISCON '02. Proceedings. IEEE*, volume 1, pages 122–128, Aug 2002. 3

[10] S. B. Jemaa, M. Hammami, and H. Ben-Abdallah. Data-mining process: application for hand detection in contact free settings. *Image Processing*, 7(8):742–750, November 2013. 1

[11] S. K. Kang, M. Y. Nam, and P. K. Rhee. Color based hand and finger detection technology for user interaction. In *Proceedings of the International Conference on Convergence and Hybrid Information Technology*, pages 229–236, Aug 2008. 1

[12] H. C. V. Lakshmi and S. PatilKulakarni. Segmentation algorithm for multiple face detection for color images with skin tone regions. In *Signal Acquisition and Processing, 2010. ICSAP '10. International Conference on*, pages 162–166, Feb 2010. 3

[13] S. Marcel. Hand posture recognition in a body-face centered space. In *Proceedings of the Conference on Human Factors in Computer Systems (CHI)*, CHI EA '99, pages 302–303, New York, NY, USA, 1999. ACM. 3

[14] G. Marin, F. Dominio, and P. Zanuttigh. Hand gesture recognition with leap motion and kinect devices. In *Image Processing (ICIP), 2014 IEEE International Conference on*, pages 1565–1569, Oct 2014. 3

[15] J. Nalepa, T. Grzejszczak, and M. Kawulok. Wrist localization in color images for hand gesture recognition. In D. A. Gruca, T. Czachórski, and S. Kozielski, editors, *Man-Machine Interactions 3*, volume 242 of *Advances in Intelligent Systems and Computing*, pages 79–86. Springer International Publishing, 2014. 3

[16] P. Prasertsakul and T. Kondo. A fingertip detection method based on the top-hat transform. In *11th International Conference on Electrical Engineering/Electronics, Computer, Telecommunications and Information Technology (ECTI-CON)*, pages 1–5, May 2014. 1

[17] Z. Ren, J. Yuan, J. Meng, and Z. Zhang. Robust part-based hand gesture recognition using kinect sensor. *Multimedia, IEEE Transactions on*, 15(5):1110–1120, Aug 2013. 1

[18] D. L. Ruderman and W. Bialek. Statistics of natural images: Scaling in the woods. *Physical Review Letters*, 73:814–817, Aug 1994. 2